

# Fingerprints of the magnetic polaron in nonequilibrium electron transport through a quantum wire coupled to a ferromagnetic spin chain

Frank Reininghaus, Thomas Korb, and Herbert Schoeller

*Institut für Theoretische Physik, Lehrstuhl A,  
Rheinisch-Westfälische Technische Hochschule Aachen,  
52056 Aachen, Germany*

(Dated: December 2, 2024)

We study nonequilibrium quantum transport through a mesoscopic wire coupled via local exchange to a ferromagnetic spin chain. Using the Keldysh formalism in self-consistent Born approximation we identify fingerprints of the magnetic polaron state formed by hybridization of electronic and magnon states. Due to its low decoherence rate, we find coherent transport signals. Both elastic and inelastic peaks of the differential conductance are discussed as function of external magnetic fields, the polarization of the leads and the electronic level spacing of the wire.

PACS numbers: 73.23.-b, 75.10.Jm, 75.75.+a, 72.25.-b

*Introduction.* In recent years, the field of Spintronics has attracted increasing interest [1, 2]. A considerable amount of theoretical and experimental attention has been focused on transport phenomena, especially spin-dependent charge currents in low-dimensional structures made of magnetic materials [3, 4, 5], but also transport of magnetization through insulating spin chains and quantum dots [6, 7].

In this Letter, we study the interplay between nonequilibrium electron transport and magnetic degrees of freedom in a one-dimensional system. The model under consideration is a finite quantum wire which is coupled via local exchange to a one-dimensional ferromagnetic Heisenberg spin chain and via tunneling to two large (spin-polarized) electronic reservoirs. Examples of one-dimensional systems which exhibit ferromagnetic coupling of localized spins are so-called ‘sandwich clusters’ formed from vanadium and benzene [8, 9, 10]. Usually, one would expect that emission of magnons in the spin chain will lead to a relaxation and dephasing of the electron spins antiparallel to the spin direction of the spin chain, leading to incoherent spin transport for this spin direction. However, from several works on ferromagnetic semiconductors [11, 12, 13, 14] it is well known, that a single electron with antiparallel spin direction to the localized spins can hybridize with one-magnon states to form the so-called *magnetic polaron* states. These states form a band which is separated from the band of scattering states, and therefore, have a low decoherence rate. It is the aim of the present paper to find fingerprints of these states in coherent transport signals at low temperatures by studying the differential conductance as function of bias voltage. We note that one-electron scattering in finite quantum spin chains has been studied in Ref. [4] at low temperatures with the result of an interesting resonance structure as function of the Fermi level. However, this work was restricted to linear transport, so that only states near the Fermi level contributed to transport. Therefore, the influence of the magnetic po-

laron states (lying outside the band of scattering states) was not probed there.

We calculate the differential conductance  $G = \frac{dI}{dV}$  for large ( $N = 1000$  sites) and small ( $N = 12$ ) systems which differ in the electronic level spacing. We find peak structures which are due to elastic and inelastic transport processes. Parameters like the external magnetic field, the spin polarizations of the leads and the bias voltage affect the energies and decay rates of the electronic states of the system. One can thus control the position and height of the peaks in the differential conductance and identify the processes which contribute to the current.

*Hamiltonian.* We employ a tight-binding model for the quantum wire and a Heisenberg model with ferromagnetic coupling  $J > 0$  for the spin chain. Both have the same lattice constant  $a$ . An external magnetic field causes Zeeman splittings  $h_e$  and  $E_Z$  for electrons in the wire and for localized spins in the chain, respectively:

$$H_{\text{wire}} = -t \sum_{i\sigma} \left( c_{i\sigma}^\dagger c_{i+1\sigma} + \text{h.c.} \right) + \frac{1}{2} h_e \sum_{i\sigma} \sigma c_{i\sigma}^\dagger c_{i\sigma}$$

$$H_{\text{spin}} = -J \sum_i \mathbf{S}_i \mathbf{S}_{i+1} + E_Z \sum_i S_i^z$$

with  $\sigma = \pm$  (we will frequently write  $\sigma = \uparrow$  or  $\sigma = \downarrow$  instead). We consider low electron densities in the wire

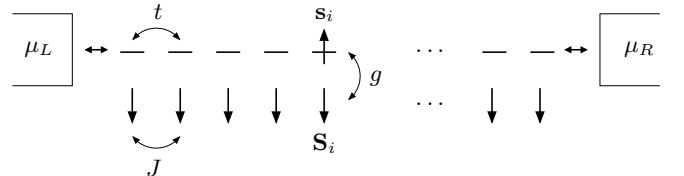


FIG. 1: The model under consideration. The conduction electrons can hop between neighboring sites in the wire, and the localized spins are coupled ferromagnetically. There is a local coupling between the spin of the conduction electrons and the localized spin at each site. The wire is coupled to two leads with the chemical potential  $\mu_L$  and  $\mu_R$ , respectively.

and therefore neglect the Coulomb interaction.

We follow [12] and use the Holstein-Primakoff transformation [15] to replace the spin operators in the chain by boson operators  $b_i^\dagger, b_i$ :

$$S_i^+ \approx \sqrt{2S} b_i^\dagger, \quad S_i^- \approx \sqrt{2S} b_i, \quad S_i^z = b_i^\dagger b_i - S \quad (1)$$

This approximation is valid if the spin chain is close to its ferromagnetic ground state where  $\langle S_i^z \rangle = -S$ . The Zeeman energy  $E_Z$  must be sufficiently large to ensure that this is the case.

Using periodic boundary conditions, we can write

$$H_{\text{wire}} = \sum_{k\sigma} \varepsilon_{k\sigma} c_{k\sigma}^\dagger c_{k\sigma}, \quad H_{\text{spin}} = E_0 + \sum_k \omega_k b_k^\dagger b_k$$

where  $E_0 = -NJS^2 - NSE_Z$  is the ground state energy of the spin chain,  $b_k^\dagger$  and  $b_k$  are creation and annihilation operators for magnons, and

$$\varepsilon_{k\sigma} = -2t \cos(ka) + \frac{1}{2} \sigma h_e, \quad \omega_k = 2JS(1 - \cos(ka)) + E_Z$$

are one-electron and one-magnon energies, respectively. If  $E_Z \gg JS$ , we can assume that the magnon energies are independent of the wave number:  $\omega_k \approx \omega = E_Z$ . We assume that the occupation of magnon states is always equal to the equilibrium occupation  $n(\omega) = (\exp(\beta\omega) - 1)^{-1}$ , i.e. that there is a strong relaxation caused by the coupling to an external spin bath.

The local interaction  $V = g \sum_i \mathbf{s}_i \mathbf{S}_i$  between electron spins  $\mathbf{s}_i$  and localized spins  $\mathbf{S}_i$  is transformed using (1) to  $V = V^{(1)} + V^{(2)} + \Delta$ , where

$$V^{(1)} = g \sqrt{\frac{S}{2N}} \sum_{kq} \left( b_q^\dagger c_{k-q\downarrow}^\dagger c_{k\uparrow} + b_q c_{k+q\uparrow}^\dagger c_{k\downarrow} \right)$$

corresponds to spin flips of a conduction electron which involve the emission or absorption of a magnon,  $V^{(2)} = \frac{g}{2N} \sum_{kqq'\sigma} \sigma b_{q+q'}^\dagger b_q c_{k-q'\sigma}^\dagger c_{k\sigma}$  implicates electron-magnon scattering, and  $\Delta$  is a spin-dependent energy shift which can be combined with  $\varepsilon_{k\sigma}$  to form a new one-electron energy  $\bar{\varepsilon}_{k\sigma} = -2t \cos(ka) + \frac{1}{2} \sigma (h_e - gS)$ .

Tunneling of electrons into and out of the leads is taken into account by a term  $H_T = \sum_{\alpha l k \sigma} \left( t_\sigma^\alpha a_{\alpha l \sigma}^\dagger c_{k\sigma} + \text{h.c.} \right)$ . Here,  $\alpha \in \{\text{L}, \text{R}\}$  labels the left or right lead and  $l$  the electronic states with energies  $\varepsilon_{\alpha l \sigma}$  in the respective lead. The leads are assumed to be noninteracting and to have a constant, but possibly spin-dependent, density of states. This is reflected in the energy-independent coupling function  $\Gamma_\sigma^\alpha = \Gamma_\sigma^\alpha(E) = 2\pi \sum_l t_\sigma^\alpha t_\sigma^{\alpha*} \delta(E - \varepsilon_{\alpha l \sigma})$ .

*Method.* The nonequilibrium Green's function method proposed by Keldysh [16] is used to calculate the current through the wire. The current can be expressed in terms of the Green's functions using a formula developed in [17]. We divide the electron self-energy into two parts  $\Sigma =$

$\Sigma_T + \Sigma_M$  where  $\Sigma_T$  is due to the tunneling term  $H_T$  and  $\Sigma_M$  is the contribution of the electron-magnon interaction  $V$ . The retarded, advanced and Keldysh component of  $\Sigma_T$  can be expressed in terms of the coupling function  $\Gamma_\sigma^\alpha$ :

$$\Sigma_{T\sigma}^{\text{R,A}} = \mp \frac{i}{2} \Gamma_\sigma, \quad \Sigma_{T\sigma}^{\text{K}}(E) = i \sum_\alpha \Gamma_\sigma^\alpha (2f_\alpha(E) - 1)$$

where  $\Gamma_\sigma = \sum_\alpha \Gamma_\sigma^\alpha$  and  $f_\alpha(E)$  is the Fermi function for lead  $\alpha$  which has the chemical potential  $\mu_\alpha$ .

The self-energy contribution  $\Sigma_M$  is calculated in self-consistent Born approximation (which corresponds to the consideration of diagrams of the order  $\mathcal{O}(g^2)$ ). We evaluate  $\Sigma_M$  using free magnon Green's functions which do not depend on the magnon wave number due to the approximation  $\omega_k \approx \omega$ . Therefore,  $\Sigma_M$  is independent of the electron wave number. With  $M_\sigma(E) = \sum_k |G_{k\sigma}^{\text{R}}(E)|^2$ , its imaginary part is given by

$$\text{Im } \Sigma_{M\sigma}^{\text{R}}(E + \sigma\omega) = -\frac{g^2 S}{4N} M_{-\sigma}(E) \sum_\alpha \Gamma_{-\sigma}^\alpha f_\alpha^{-\sigma}(E), \quad (2)$$

where  $f_\alpha^+ = f_\alpha$ ,  $f_\alpha^- = 1 - f_\alpha$ . The real part is obtained from the Kramers-Kronig relations. Terms which are proportional to the occupation  $n(\omega)$  of magnon states have been omitted because  $n(\omega) \ll 1$  for the parameters chosen in the next section [18]. Dyson's equation and (2) are solved self-consistently using an iterative procedure [19].

While a more general set of diagrams involving an arbitrary number of electron-magnon scattering vertices between the emission and absorption vertices yields the exact  $\uparrow$ -electron self-energy in the special case which was considered by Richmond [12], we disregard all contributions of higher order than  $\mathcal{O}(g^2)$  because they would give rise to terms in the nonequilibrium current which violate charge conservation (i.e. the sum of the currents from the leads would be non-zero:  $I_L + I_R \neq 0$ ). This problem could be solved if another set of more complex self-energy diagrams was taken into consideration additionally. The discussion of a charge-conserving approximation for the self-energy involving higher-order diagrams will be addressed in a future publication, but does not change the qualitative effects discussed in this work.

There are two contributions to the current through the wire: Electrons which tunnel into the system from lead  $\alpha$  with spin  $\sigma$  can either tunnel to lead  $\alpha'$  with unchanged spin  $\sigma$  (elastic current) or flip their spin by emitting or absorbing a magnon and leave the system with spin  $-\sigma$  (inelastic current). The elastic and inelastic current con-

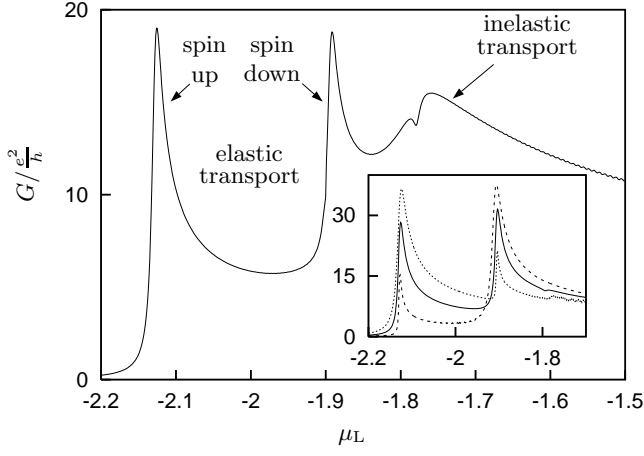


FIG. 2: Differential conductance for a system with  $N = 1000$  sites and  $S = 1/2$ . The parameters are  $t = 1$ ,  $g = 0.5$ ,  $E_Z = h_e = 0.1$ ,  $k_B T = 5 \times 10^{-4}$ ,  $\sum_{\sigma} \Gamma_{\sigma}^{L,R} = 10^{-2}$ ,  $P_L = +0.7$ ,  $P_R = -0.7$ . The chemical potential  $\mu_R$  of the right lead is fixed at  $-2.5$ . **Inset:** Conductance for unpolarized leads (solid line) and ferromagnetic leads with parallel polarization and  $P = +0.7$  (dotted line),  $P = -0.7$  (dashed line).

tributions for lead  $\alpha$  are

$$I_{\alpha}^{\text{el}} = \frac{e}{h} \int dE \sum_{\alpha'} \sum_{\sigma} T_{\alpha\alpha'\sigma}^{\text{el}}(E) (f_{\alpha}(E) - f_{\alpha'}(E)),$$

$$I_{\alpha}^{\text{inel}} = \frac{e}{h} \int dE \sum_{\alpha'} \left( T_{\alpha\alpha'}^{\text{inel}}(E) f_{\alpha}(E) [1 - f_{\alpha'}(E - \omega)] \right. \\ \left. + T_{\alpha\alpha'}^{\text{inel}}(E) [1 - f_{\alpha}(E - \omega)] f_{\alpha'}(E) \right),$$

where we have again neglected terms  $\propto n(\omega)$ . The transmission coefficients are given by

$$T_{\alpha\alpha'\sigma}^{\text{el}}(E) = \Gamma_{\sigma}^{\alpha} \Gamma_{\sigma}^{\alpha'} M_{\sigma}(E), \quad (3)$$

$$T_{\alpha\alpha'}^{\text{inel}}(E) = \frac{g^2 S}{2N} \Gamma_{\uparrow}^{\alpha} \Gamma_{\downarrow}^{\alpha'} M_{\uparrow}(E) M_{\downarrow}(E - \omega). \quad (4)$$

We consider both nonmagnetic leads and spin-polarized ferromagnetic leads. Their polarization is measured by  $P_{\alpha} = (\Gamma_{\uparrow}^{\alpha} - \Gamma_{\downarrow}^{\alpha}) / (\Gamma_{\uparrow}^{\alpha} + \Gamma_{\downarrow}^{\alpha})$ .

**Results.** The differential conductance for a large system with  $N = 1000$  sites where the level spacing is smaller than the other relevant energy scales is shown in Fig. 2. Since the electron density in the wire should be sufficiently low to justify the neglect of the Coulomb interaction, we examine the voltage regime where only a small fraction of the  $\uparrow$ - and  $\downarrow$ -electron states is partially occupied. We fix  $\mu_R$  below the conduction band at  $\mu_R = -2.5$  and vary  $\mu_L$ .

For low bias voltages ( $\mu_L \lesssim -1.85$ ), elastic transport processes dominate. They correspond to resonances of  $|G_{k\sigma}^R(E)|^2$  whose broadening is not dominated by the electron-magnon interaction. One peak at  $\mu_L \approx -2.12$  for spin up is due to the magnetic polaron band, and the

other at  $\mu_L \approx -1.89$  corresponds to spin down electrons, which are parallel to the localized spins and, therefore, cannot be flipped in the absence of magnons at low temperatures. The shape of the peak structures reflects the density of states in a one-dimensional system. Inelastic processes superpose these structures. In the situation where  $P_L = +0.7$  and  $P_R = -0.7$  (main plot of Fig. 2), they dominate for higher voltages ( $\mu_L \gtrsim -1.85$ ). The reason is that this set-up favors inelastic transport because it maximizes the product  $\Gamma_{\uparrow}^L \Gamma_{\downarrow}^R$  of the coupling functions which is proportional to the inelastic transmission coefficient (4). The inset of Fig. 2 shows how the different peaks can be distinguished by changing the spin polarization of the leads. Here, three conductance curves are shown for unpolarized leads and ferromagnetic leads with parallel polarizations ( $P_L = P_R = P$ , where  $P = +0.7$  or  $P = -0.7$ ). The weight of the peak structure which is related to elastic transport of electrons with spin  $\sigma$  is greatest if the leads are  $\sigma$ -polarized ( $\sigma \in \{\uparrow, \downarrow\}$ ), just as one would expect. While there is also an inelastic current contribution in these configurations, it does not cause a clear signal in the differential conductance.

For a small system with  $N = 12$  sites, the discrete structure of the energy spectrum can be identified in the differential conductance. This is the case if the level spacing  $\Delta E$  is larger than the energy scales  $\Gamma$  and  $k_B T$  which determine the broadening of the conductance peaks. In the considered voltage regime, only the lowest electronic states (wave number  $k = 0$ , spin  $\uparrow$  or  $\downarrow$ ) are partially occupied and contribute to the current. The electronic spin up states are split mainly by the  $q = 0$  magnon into two states with energy  $\tilde{\epsilon}_{\uparrow}$  and  $\tilde{\epsilon}_{\uparrow}'$  (corresponding to the magnetic polaron state and the scattering state in the continuum case, respectively). Furthermore, the electronic spin down states are also renormalized to  $\tilde{\epsilon}_{\downarrow}$  when the  $\uparrow$ -electron states have a finite occupation probability.

Results for  $g > 0$  (antiferromagnetic local exchange coupling) are presented in Fig. 3. As in the situation discussed above, conductance peaks which are due to elastic transport processes coincide with resonances of the retarded Green's functions. Here, the left and right large peak occur at  $\tilde{\epsilon}_{\uparrow}$  and  $\tilde{\epsilon}_{\downarrow}$ , the main resonances of the  $\uparrow$ - and  $\downarrow$ -electron Green's function (with wave number  $k = 0$ ), respectively, and can be attributed to elastic transport through the wire. On the other hand, the inelastic transmission coefficient (4) is proportional to both  $|G_{\uparrow}^R(E)|^2$  and  $|G_{\downarrow}^R(E - \omega)|^2$ . Therefore, inelastic transport processes contribute to the differential conductance at  $\mu_L = \tilde{\epsilon}_{\uparrow}$  (where some weight is added to the left large peak) and  $\mu_L = \tilde{\epsilon}_{\downarrow} + \omega$ , the position of the smaller peak. The dependence of the relative peak heights on the lead polarizations is like in the large system discussed above.

Actually, one could expect another peak in Fig. 3 because the  $\uparrow$ -electron Green's function has a second resonance at an energy  $\tilde{\epsilon}_{\uparrow}'$ . However, this resonance has in

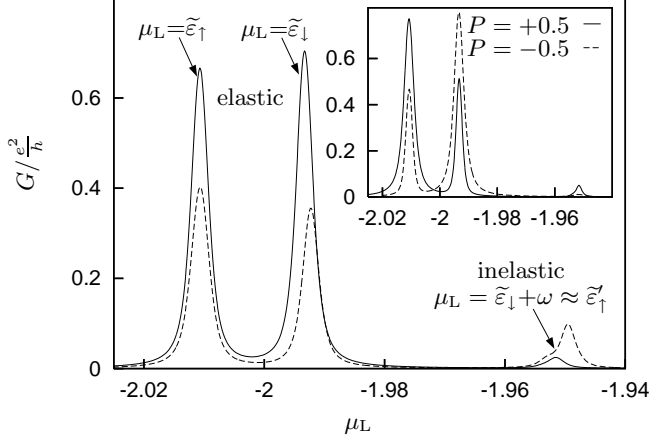


FIG. 3: Conductance for  $N = 12$ ,  $S = 1/2$ . The parameters are:  $t = 1$ ,  $g = 0.1$ ,  $E_Z = h_e = 0.04$ ,  $k_B T = 5 \times 10^{-4}$ ,  $\sum_{\sigma} \Gamma_{\sigma}^{L,R} = 2 \times 10^{-3}$ ,  $\mu_R = -2.5$ . Both nonmagnetic leads (solid line) and spin-polarized ferromagnetic leads with  $P_L = +0.7$ ,  $P_R = -0.7$  (dashed line) are considered. **Inset:**  $G$  for ferromagnetic leads with parallel polarization.

general quite a small weight because the magnitude of the imaginary part of the  $\uparrow$ -electron self-energy is rather large at  $\tilde{\epsilon}_{\uparrow}^{\uparrow}$ , leading to a strong decay of the corresponding state and a suppression of elastic transport. Moreover,  $\tilde{\epsilon}_{\uparrow}^{\uparrow}$  is very close to the energy  $\tilde{\epsilon}_{\downarrow} + \omega$  where inelastic transport contributes to the differential conductance. Therefore, elastic transport of  $\uparrow$ -electrons is visible only at  $\tilde{\epsilon}_{\uparrow}$  (energy of the magnetic polaron state), the small contribution at  $\mu_L = \tilde{\epsilon}_{\uparrow}^{\uparrow}$  is absorbed in the 'inelastic' peak.

It should be noted that not only the peak heights, but also the positions depend on the polarizations of the leads. Fig. 3 shows that the peak at  $\mu_L = \tilde{\epsilon}_{\downarrow}$  and the inelastic peak are shifted to the right for the configuration where the leads have antiparallel polarizations. The reason is that a  $\downarrow$ -electron (or hole) can only interact with magnons by flipping its spin and occupying a  $\uparrow$ -state. Therefore, the  $\downarrow$ -electron self-energy (and thus the position  $\tilde{\epsilon}_{\downarrow}$  of the main resonance of the Green's function) depends on the occupation probability of  $\uparrow$ -electron states. This probability is given by  $F_{\uparrow}(E) \approx \sum_{\alpha} \frac{\Gamma_{\uparrow}^{\alpha}}{\Gamma_{\uparrow}} f_{\alpha}(E)$  for a state with energy  $E$  and is affected by both the chemical potentials and the polarizations of the leads.

Conductance curves for ferromagnetic local exchange coupling ( $g < 0$ ) and different magnetic fields are shown in Fig. 4. The Zeeman splitting  $E_Z$  of the localized spins is chosen to be twice as large as the splitting  $h_e$  of the conduction electrons. Therefore, not only the peak positions, but also the general structure of the conductance curve changes if the magnetic field is varied. For small ( $h_e \approx 0.02$ ) and large ( $h_e \approx 0.06$ ) fields, the situation is comparable to Fig. 3: There are two large 'elastic' peaks at  $\mu_L = \tilde{\epsilon}_{\uparrow}$  and  $\mu_L = \tilde{\epsilon}_{\downarrow}$  and a small 'inelastic' peak at  $\mu_L = \tilde{\epsilon}_{\downarrow} + \omega$ . These peaks move with different

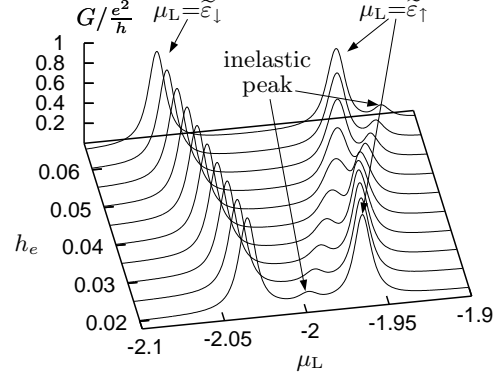


FIG. 4: Conductance for  $t = 1$ ,  $g = -0.1$ ,  $k_B T = 10^{-3}$ ,  $\Gamma_{\sigma}^{L,R} = 5.5 \times 10^{-3}$ ,  $\mu_R = -2.5$ . The Zeeman splittings  $h_e$  for conduction electrons and  $E_Z = 2h_e$  for localised spins are different for each curve.

'velocities' if the field is increased: The positions of the large peaks, i.e. of the main resonances of the retarded Green's functions, change with the conduction electron Zeeman energy  $\pm h_e/2$ , but the position of the inelastic peak changes like  $-h_e/2 + E_Z = 3/2 h_e$  because of our choice  $E_Z = 2h_e$ . One could expect that the inelastic and the right elastic peak overlap and form a single resonance for intermediate fields ( $h_e \approx 0.045$ ), but this is not the case. The corresponding conductance curve rather reveals two peaks of comparable height. These arise from two resonances of the  $\uparrow$ -electron Green's function which have approximately equal weight for this particular set of parameters. This means that the decoherence rates are equal for the states corresponding to the energies  $\tilde{\epsilon}_{\uparrow}$  and  $\tilde{\epsilon}_{\uparrow}^{\uparrow}$ , in contrast to the situation in Fig. 3. Elastic transport of  $\uparrow$ -electrons thus generates a double-peak structure in the differential conductance. It is superposed by the inelastic transport contribution, but this does not change the structure qualitatively.

*Summary.* We presented a self-consistent diagrammatic approach within the Keldysh formalism to calculate the nonequilibrium current through a mesoscopic quantum wire coupled to a ferromagnetic spin chain. We proposed a way to detect the coherent superposition of electronic and magnon states, the so-called magnetic polaron state. It shows up as a high (i.e. coherent) signal in the differential conductance and can be tuned by external magnetic fields and the spin polarization in the leads. In this way we have shown that the interaction between electrons and magnons (which usually leads to unwanted relaxation and dephasing of the electron spin) can be used for the creation of a phase-coherent quantum state. Therefore, we expect that this work will stimulate further theoretical and experimental investigations of the magnetic polaron state in the field of mesoscopic systems.

*Acknowledgements.* The authors would like to thank

S. Jakobs and J. König for helpful discussions. This work has been supported by the VW Foundation and the Forschungszentrum Jülich (via the virtual institute IFMIT).

- 
- [1] S. A. Wolf, D. D. Awschalom, R. A. Buhrman, J. M. Daughton, S. von Molnár, M. L. Roukes, A. Y. Chtchelkanova, and D. M. Treger, *Science* **294**, 1488 (2001).
  - [2] I. Žutić, J. Fabian, and S. Das Sarma, *Rev. Mod. Phys.* **76**, 323 (2004).
  - [3] V. Rodrigues, J. Bettini, P. C. Silva, and D. Ugarte, *Phys. Rev. Lett.* **91**, 096801 (2003).
  - [4] Y. Avishai and Y. Tokura, *Phys. Rev. Lett.* **87**, 197203 (2001).
  - [5] C. Gould, A. Slobodskyy, T. Slobodskyy, P. Grabs, and D. Supp (2005), cond-mat/0501597.
  - [6] F. Meier and D. Loss, *Phys. Rev. Lett.* **90**, 167204 (2003).
  - [7] O. Strelcyk, T. Korb, and H. Schoeller, *Phys. Rev. B* **72**, 165343 (2005).
  - [8] K. Miyajima, A. Nakajima, S. Yabushita, M. B. Knickelbein, and K. Kaya, *J. Am. Chem. Soc.* **126**, 13202 (2004).
  - [9] J. Wang, P. H. Acioli, and J. Jellinek, *J. Am. Chem. Soc.* **127**, 2812 (2005).
  - [10] H. S. Kang, *J. Phys. Chem. A* **109**, 9292 (2005).
  - [11] S. Methfessel and D. C. Mattis, in *Handbuch der Physik*, edited by S. Flügge (Springer-Verlag, Berlin, 1968), vol. XVIII/1, pp. 419–424.
  - [12] P. Richmond, *J. Phys. C* **3**, 2402 (1970).
  - [13] B. S. Shastry and D. C. Mattis, *Phys. Rev. B* **24**, 5340 (1981).
  - [14] W. Nolting, *Phys. Status Solidi B* **96**, 11 (1979).
  - [15] R. Holstein and H. Primakoff, *Phys. Rev.* **58**, 1098 (1940).
  - [16] L. V. Keldysh, *Soviet Physics JETP* **20**, 1018 (1965).
  - [17] Y. Meir and N. S. Wingreen, *Phys. Rev. Lett.* **68**, 2512 (1992).
  - [18] Note that the low occupation  $n(\omega) \ll 1$  of magnon states ensures the validity of the Holstein-Primakoff transformation (1).
  - [19] We remark that a non-self-consistent solution (which corresponds to stopping the procedure after the first iteration) yields qualitatively different results.